Published on the Journal of the European Ceramic Society, 28 (2008) 169–176 © by Elsevier Ltd DOI 10.1016/j.jeurceramsoc.2007.06.014

Heterocoagulation-spray drying process for the inclusion of ceramic pigments

A.L. Costa[a], F. Matteucci[a], M. Dondi[a,*], I. Zama[b], S. Albonetti[b], G. Baldi[c]

[a]*ISTEC-CNR, Institute of Science and Technology for Ceramics, Via Granarolo 64, 48018 Faenza, Italy*
[b]*Department of Industrial and Materials Chemistry, University of Bologna, Viale Risorgimento 4, 40136 Bologna, Italy*
[c]*CE.RI.COL., Colorobbia Research Centre, Via Pietramarina 53, 50053 Sovigliana-Vinci, Italy*

Abstract

The improvement of the physico-chemical resistance of hematite pigment in ceramic bodies has been pursued through its inclusion into a transparent and refractory matrix of silica or zirconia. The inclusion process was accomplished by heterocoagulation followed by spray-drying. The heterocoagulation process was optimised through an electrokinetic technique, that measured the zeta potential of both matrix and pigment as a function of pH and of different amounts of dispersing agents. Suspensions of pigment and matrix were designed in order to achieve the maximum surface charges. The heterocoagulated mix was then spray-dried in order to avoid any separated coagulation of pigment and matrix and to obtain a well granulated powder suitable for application in ceramic bodies. A stable red-coloured ceramic pigment for low firing applications was obtained starting from amorphous silica as matrix and hematite as colorant.

Keywords: Ceramic pigments; Electroacoustic spectroscopy; Hetero-coagulation; Optical properties; Powders-chemical preparation; Surface properties; X-ray diffraction.

1. Introduction

A ceramic pigment is an inorganic compound that colours the ceramic wares without reacting with the body or the glaze in which it is dispersed.[1-2] Although many inorganic compounds can act as pigment, only few of them are suitable for colouring ceramic wares, due to the high firing temperature and chemical aggressiveness of ceramic bodies and glazes that cause the pigment dissolution.[3-4] The technological performance of a ceramic pigment can be improved by including it in a transparent and inert matrix. These composites, called heteromorphic pigments, behave like a single chromatic unit into ceramic bodies or glazes, and their colour is given by the pigment crystals that are occluded into the transparent matrix.[5]

Among ceramic pigments, there is a restricted choice for red/orange colours, as the current products give hues far away from the pure red. The most common are the cadmium sulpho-selenide pigments that develop an intense red colour, but present both technological and environmental problems, due to their low thermal stability and to the high toxicity of Cd and Se.[6-7] Inclusion of cadmium sulpho-selenide inside a zircon matrix ($ZrSiO_4$) has been industrially achieved but involves a very expensive process.[8-9] In order to assess new ways for including a ceramic pigment into an inert matrix, different wet chemical processes have been recently developed, such as sol-gel and chemical co-precipitation,[10-17] but no industrial scale-up is known at present.

The aim of this work is to include hematite into silica or zirconia matrices using a wet chemical process. Hematite is the most important red pigment in many applications,[18] but its use as ceramic colorant is precluded by solid (or liquid-solid) state transformations that lead to the dissolution of the iron oxide into ceramic bodies or glazes. This process causes

a significant colour change colour already at 1000 °C, that is a temperature too low for most current ceramic firing processes. Zirconia and amorphous silica were chosen as inert matrix due to their thermal and chemical stability towards glassy phases and low cost. Besides, there is a naturally-occurring pigment, known as Gres de Thiviers, successfully used for colouring ceramic bodies and/or glazes, that is made of hematite occluded in quartz grains.[19-20] In order to get hematite-silica and hematite-zirconia composites, an innovative two-steps process was designed and experimented:[21]

1) mixing the pigment and matrix suspensions once the maximum surface charges attraction was achieved (heterocoagulation);
2) spray-drying of the heterocoagulated mixture (atomization).

Chemico-physical and technological characterizations of both semi-finished and finished products were performed in order to understand the inclusion mechanism and to evaluate the process efficiency.

2. Experimental

2.1. Powder and processing

The reagents used in this work are summarized in Table 1.

Heterocoagulation: the surface of hematite dispersed in water was functionalized with either Primene (5 wt.%) or Duramax (1.4 wt.%). The colloidal silica was used as received from the manufacturer. The $Zr(OH)_4$ suspension was stabilized with Primene (10 wt.%). The hematite:matrix suspensions (weight ratio 1:5) plus additives were acidified at pH 3 with 1*M* HCl (Carlo Erba, Italy) and ball milled for about 20h before mixing. The heterocoagulation was carried out by mixing suspensions of hematite and inert matrix in a pH range (from 3 to 5) where surfaces have opposite charges. For precursor suspensions, the optimal pH value was chosen on the basis of ξ Z potential measurements, while the effective pH of heterocoagulation is reported in Table 2. All the mixtures, if not differently indicated, were designed to keep the hematite/inert matrix ratio equal to 1/5 and a total solid content of 30 wt.%. Different suspensions were prepared and labeled as presented in Table 2.

Spray-drying: once prepared, the heterocoagulated suspensions were spray-dried in a lab atomizer. To verify the effect of spray drying process on the material, sample H1 was separated from the liquid by decantation and dried in oven (105°C overnight).

The mixtures of hematite and inert matrix were pumped in the hot chamber of a laboratory spray drier (Mod. SD-05, Lab-Plant Ltd., UK). The following parameters proved to be the best to achieve the maximum process-yield: co-current flow, pump suction flow: 210 cm^3/h; air flow: 65 m^3/h; atomising air pressure: 1.8 bar; nozzle diameter: 1.5 mm; air stream temperature: 200 °C.

Firing: The spray dried powders obtained from the mixtures A and E were fired (maximum temperature in between 950-1300°C) in order to evaluate the effect of a firing treatment on the pigment-matrix adhesion. Both formulation and processing of iron oxide pigments included in silica or zirconia matrices are summarized in Table 3. In order to verify the efficiency of this new two-steps process, dry mechanical mixtures were prepared by mixing the precursor powders in an automatically-driven agata mortar (samples M1, M2, M3). In particular, the amorphous silica utilized for M1 mechanical mixing was obtained by drying the Ludox PX-30 suspension.

2.2 Characterization

Electroacoustic characterization: an Acoustosizer II (Colloidal Dynamics, Sydney, Australia) was used to determine the ξ potential of concentrated colloidal suspensions. The electroacoustic effect measured is the ESA (electrokinetic sonic amplitude) referred to the sound wave generated when an alternating electric field is applied to a colloidal suspension. The ESA signal gives information on the dispersive state of the suspension, being proportional to the dynamic mobility of the particles and as consequence to their electrokinetic potential (ξ potential).[22] The Acoustosizer measures the ESA response of dispersed colloidal particles over a set of thirteen frequencies ranging from 1 to 18 MHz (ESA spectrum). The software associated derives the dynamic mobility spectrum and extracts reliable values of ξ potential and particle size, fitting the experimental spectrum with the theoretical one based on a mathematical model developed by O'Brien.[23-24] The particle-size distribution, necessary for the fitting, is measured by a sound attenuation technique that gives reliable values of particle size independently on dynamic mobility response. Temperature, pH and electric conductivity data of the suspension are collected during the measurement. A potentiometric titration software allowed the addition of acid or base (1M KOH and 1M HCl, Carlo Erba, Italy) according to the pH increments set in the experimental set up. A concentration titration software governed the addition of the amount of dispersant. In both cases an equilibrium delay time (1-2 minutes) before each measurement was set. The aqueous slurries were prepared by ultrasonic mixing for 1 hour, fixing the electrolyte strength with 10 mM of KCl (Merck) and with a solid concentration of 5wt.%. The automatic titration software was used to measure ξ potential as a function of pH and amount of additives in order to find the point of zero ξ potential, called isoelectric point (pH_{iep}), and the optimal amount of additives required.

Chemico-physical characterization: the chemical composition of the included pigment was determined by Inductively Coupled Plasma-Atomic Emission Spectrometry (ICP-AES, Liberty 200, Varian, Australia). The samples were melted in graphite crucible with lithium tetraborate at 1200°C. Powder morphology was investigated by scanning electron microscopy (SEM, Leica Cambridge Stereoscan 360, UK) coupled with an energy-dispersive X-ray spectrometer (EDX, Link Analytical eLX, UK). UV-visible-NIR spectroscopy was performed by diffuse reflectance with integrating sphere (λ 35, Perkin Elmer, USA) in the 300-1100 nm range, step 0.3 nm, using $BaSO_4$ as a reference. The phase composition of the samples was investigated through laboratory X-ray powder diffraction (Philips PW1820/00 goniometer using graphite-monochromated Cu $K\alpha_{1,2}$ radiation, 15-130 °2θ measuring range, scan rate 0.02 °2θ , 10 s per step). Rietveld crystal structure refinement of the M2 and M3 pigments was performed (Fig. 1) in order to evaluate the chemical inertia of ZrO_2 towards hematite.[25-26] Starting atomic parameters for zirconia were taken from Gualtieri and co-workers,[27] considering $P2_1/c$ as the space group. Depending upon the number of impurities up to 35 independent variables were refined: zero-point, 10 coefficients of the shifted Chebyschev function to fit the background, scale factor and cell dimensions of hematite (the only accessory phase), scale factor, cell dimensions, atomic positions, site occupancies, isotropic displacement parameters of zirconia, profile coefficients - 1 gaussian (GW) and 2 lorentzian terms (LX, LY) - for both phases. The Zr versus Fe fraction in the cation site of the zirconia structure was refined by contrasting their X-ray scattering curves and assuming full occupancy of this site.

Technological characterization: it was assessed by adding the pigment into different ceramic matrices: a porcelain stoneware body (PS), a glaze for floor tiles (G) and a glassy coating for wall tiles (F), characterized by an increasing degree of chemical reactivity towards ceramic pigments. Pigments M1, S1, S2, S3, C1 and C2 were tested in every

matrix, while H1 and M1 only in glazes (G and F). The pigment (3 wt.%) was added into the ceramic body by dry mixing, hand pelletisation (8% wt moisture), uniaxial pressing (40 MPa) of 25 mm-diameter disks, drying in oven (105°C) and firing in electric kiln in static air (temperatures varying from 1080°C to 1260°C). In the case of glazes, the pigment (5% wt) was wet mixed and the slip was deposited on porous ceramic tiles, then dried in oven and fired in electric kiln in static air (980 °C for F and 1200 °C for G). The chemical and physical characteristics of ceramic matrices are reported in Matteucci and co-workers.[28] Chromatic appearance and colour stability were evaluated by measuring the CIELab parameters L*, a*, b* (L*= + white, - black; a*= + red, - green; b*= + yellow, - blue) with diffuse reflectance spectroscopy (HunterLab Miniscan MSXP4000, 400-700 nm, white glazed tile reference x=31.5, y=33.3).

3. Results and discussion

3.1 Electroacoustic characterization

The electroacoustic technique was used to investigate the dispersive behaviour of pigment and inert matrix suspensions through measurements of ▪ ▪ potential. On the basis of these results, the surface forces were manipulated by controlling pH or type and amount of additives. The first aim was to maximize the repulsive energy between particles of the same type. The second to promote the attraction between pigment and matrix particles, being surrounded by opposite charges.[29]

Electroacoustic data are summarized in Table 4. As expected, both hematite and $Zr(OH)_4$ suspensions show a positive charge up to basic pH (pH_{iep} = 9.5 and 8.5, respectively); in fact, these values are typical of basic oxide surfaces that, interacting with the protons of water, become positively charged. These suspensions were not easy to handle as powders precipitated just few minutes after the preparation. The addition of HCl, although increasing the positive charge of both hematite and $Zr(OH)_4$, did not promote the stabilization, because the electrostatic repulsion between particles was not enough to balance the attractive and gravitational forces that induced particles coagulation and precipitation.

For this reason, Duramax or Primene were added in order to stabilize the suspensions and functionalize the surfaces with a negative or positive charge, respectively. The steric hindrance of large aliphatic chains of polycarboxilate (Duramax) and amine substitutes (Primene), adding a steric repulsion to the electrostatic one, resulted fundamental in order to stabilize the suspensions. As the best heterocoagulation requires suspensions with opposite charges, the hematite suspension was functionalized with Primene when mixed with silica, and with Duramax when mixed with $Zr(OH)_4$.

The colloidal silica suspensions show a negative zeta potential up to acid pH ($2 \leq pH_{iep} \leq 4$) as expected by acid oxide surfaces that transfer protons to water developing a negative charge. The plots of zeta potential as a function of pH for the three Ludox sols are reported in Figure 2. The lack of data of the PW-50 Ludox curve in the 3-5 pH range occurred because the system was not able to reach the equilibrium during the delay time set before the next measurement. Normally during this time the surface reacts exchanging protons with water and, once reached the equilibrium, the pH increases up to the set value. Difficulties of reaching the equilibrium are generally due to phenomena such as precipitation or solubilization, induced by the addition of acid. In these cases, the automatic titrator kept on adding acid until the system was totally reacted and the excess of acid added determined a jump of the pH set for the measurement. In the case of Ludox PW-50, it can be hypothesized that, starting from pH 5, the surface charge and therefore zeta potential had been totally neutralized and other phenomena, such as precipitation of soluble silicates at higher pH, occurred. For this reason the pH_{iep} value for this system was extrapolated in the middle of the pH jump. The comparison of the pH_{iep} of the three Ludox sols evidenced a shift towards acid pH passing from Ludox PX-50 to Ludox PT-40 and Ludox PX-30 that did not reach the pH_{iep} in the pH range tested. The comparison between specific surface areas of the three silica sols suggested that some soluble silicates species could be leached from the silica surfaces at high starting pH, and then specifically adsorbed into the surfaces of the silica. The concentration of these species, in fact, will be higher for higher specific surface areas (PX-30 > PT-40 > PX-50) and therefore the pH_{iep} will be shifted accordingly towards acid pH, justifying the previous assumption.[30]

The zeta potential of hematite suspension as a function of Duramax amount is shown in Figure 3A. It can be seen that positive starting zeta potential becomes negative, passing from about 5 mV to -25 mV, after the addition of about 0.3 wt.% Duramax. This indicates a good affinity of the hematite surface for Duramax, that is specifically adsorbed and

reverses the natural surface charge. Further addition of Duramax slightly increases the absolute value of zeta potential until a plateaux is reached (Duramax about 1.4 wt.%). At this point the surface is totally coated and the corresponding amount of Duramax is considered the optimum to stabilize the suspension. Any further amount of Duramax will not be adsorbed and shall affect the stability of the suspension with phenomena like the depletion flocculation.[30] Similar curves for hematite and $Zr(OH)_4$ suspensions as a function of Primene gave the best amount of additive.

3.2. Spray-drying

The efficiency of the spray-drying process, evaluated on the basis of its yield (ratio percent of spray-dried product/initial solid content), was found to be between 30% and 60%. The amount of solid loss during the process depends on the percentage of solid sticked to the walls of the spray-drier chamber and on the amount of powder eliminated with the exhausted gas. Parameters like viscosity, concentration and density of the suspension are fundamental in order to improve the process efficiency. The best yields were obtained with silica products; in particular, the Ludox PX-30 gave the best yield (62%) as a consequence of its very high surface area.

3.3. Chemical-physical characterization

An initial assessment of the efficiency of the heterocoagulation process can be gained from comparing the theoretical ratio of inclusion pigment/matrix, calculated from the initial suspension, with the ratio gained from the ICP chemical analysis in the atomized samples. Respecting the pigment/matrix ratio reflects the improved adhesion between the two phases. Chemical analyses of spray dried powders show that the matrix/hematite ratio did not change when pigment and coating suspensions were mixed and spray dried with opposite charges. On the contrary, when samples were mixed without taking account of charges, this ratio resulted very low respect to the initial one, indicating a poor adhesion. As an example, if hematite is functionalized with Duramax, instead of Primene, when mixed with colloidal SiO_2, the Fe_2O_3/SiO_2 ratio in the spray dried powder resulted 1/98 respect to 1/5. Considering the surface charge of the components concerned, in a suspension at pH 3-5 (Figure 3B), the rate of attachment of SiO_2 particles can be expected to be poor in combination with Duramax functionalized hematite (formulation F in Table 2), because both components are negatively charged. From the electrostatic point of view, an optimal rate of adhesion should be reached with positively charged hematite and this demand is ful-filled if Fe_2O_3 particles are functionalized with Primene.

The included pigments are constituted by spherical aggregates with a particle size comprised between 5 and 20 μ m (Fig. 4A and 4B). The EDS measurements show the different coatings developed by silica and zirconia matrices. In fact, hematite particles are occluded by a uniform coating of silica, while zirconia developed a non homogeneous coating. The different morphologies of agglomerates are due to the different microstructures of the inert matrices. During the drying process a solid diffusion inside the sprayed droplets occurs developing a composition gradient between the heavier particles in the inner part and the lighter particles on the surface. Thus the silica colloidal particles collapse over the coarser hematite particles, creating a homogeneous coating, while the zirconia and hematite particles fell simultaneously, due to their comparable density and size, producing a non homogeneous coating.

The only crystalline phase detected from X-ray powder diffraction in all spray dried samples was hematite: at the spray-drying maximum heating temperature (250°C) silica is present in its amorphous state. As far as the ZrO_2 coating is concerned, both samples M2

and M3 exhibit the monoclinic structure (baddeleyite). The refined occupancies of the 7-coordinated site of this structure showed a partial replacement of Zr by Fe, revealing that baddeleyite is not a suitable matrix to include hematite. This substitution is expected to favor the entrance of Fe^{3+} instead of Fe^{2+}, on the basis of ionic radii: Fe^{3+} 65 pm, Fe^{2+} 78 pm, Zr^{4+} 72 pm,[31] with the charge mismatch balanced by oxygen vacancies. However the slight increase of the cell volume with respect to that of pure m-ZrO_2 (Table 5) seems to indicate the probable contemporary presence of Fe^{3+} and Fe^{2+}. Considering the relatively low standard errors on the refined occupancies, it can be assumed that the iron fraction is reliably estimated and that the solubility of iron inside zirconia is as high as 0.10 a.p.f.u. (atoms per formula unit) in both samples (Table 5). In addition, the amount of hematite as secondary phase in both samples is directly proportional to its addition in the batch.

3.4. Technological characterization

Through-body application: The chromatic performances of silica-coated pigments in the porcelain stoneware body (PS) fired at different temperatures are shown in Figure 5. The mechanically mixed Fe_2O_3/SiO_2 pigment (M1) bestowed on PS a red hue that decreased for firing temperatures higher than 1180°C, due to the hematite dissolution in the ceramic matrix. The spray-dried pigments S1, C1 and C2, on the contrary, maintained their red colour also at temperatures over 1250°C. Furthermore, the pigments calcined at 950°C (C1) and 1100°C (C2) developed more saturated colours with respect to the not calcined sample S1 (the higher a*, the redder the colour) indicating that the calcination process enhances the thermal stability of the spray-dried pigments. In particular, the sample calcined at lower temperature (C1) has higher values of a* compared to the sample C2, which contains a significant amount of tridymite (Fig. 6) that does influence the transparency degree of the coating, so explaining the different chromatic performance of these pigments.

In addition, Figure 7 reports the different behaviour of coated pigments synthesized utilizing silica matrix with different surface area (samples S1, S2, S3). No effect was observed reducing this parameter down to 165 m^2/g (sample S2) but S3-occluded hematite showed slightly lower value of a*, indicating that silica surface area lower that 100 m^2/g could inhibit fast reaction between pigment and inert matrix.

On the contrary, the zirconia-coated sample (S5) dispersed in porcelain stoneware developed poorly saturated colour (a*=6.0, b*=2.3). This behaviour can be explained by the partial diffusion of iron into the zirconia lattice, as already shown by the XRD results.

Ceramic glaze applications: the chromatic coordinates (a* and b*) of pigments applied into ceramic glazes are reported in Figures 8 and 9. Once applied in vitreous coating fired at low temperature (980°C, Fig. 8) the mechanically mixed Fe_2O_3/SiO_2 pigment (M1) and the just heterocoagulated one (H1) developed a pale red colour (a* = 11.6 and 15.6 respectively) with an increase of the red coordinate for heterocoagulated pigment. These results confirm the importance of the process of charge functionalization carried out during heterocoagulation, that increases the adhesion between hematite and silica matrix. The spray-dried pigments, in fact, developed an intense red colour, with a* values ranging from 19 to 22. Furthermore, in this application there are not evidences of different behaviour of silica matrix with different surface area (samples S1, S2, S3), as well as of the improved amount of total solid content of heterocoagulated mixture (from 30 to 40wt.% for S1 and S4 samples, respectively) and of the calcination process following the spray-drying (samples C1 and C2). In contrast, all the pigments dissolved in the glaze for porcelain stoneware leaving the tiles colourless (Fig. 9). Both the chemical aggressiveness and the high firing temperature (1200°C) of this kind of glazes preclude the application of most silica-included hematite pigments, including the Gres de Thiviers.[20,21] Therefore, the silica matrix is suitable to prevent the dissolution of hematite at low temperatures (*i.e.* < 1100°C), whereas for higher firing temperatures further studies regarding more refractory matrices are in progress.

4. Conclusions

The inclusion of hematite into an inert matrix has been obtained by means of an innovative two-steps process involving heterocoagulation combined with spray drying. This new technology offers some remarkable advantages with respect to current procedures used in the manufacturing of included pigment: efficient way to get the pigment-matrix adhesion at low temperature; possibility to scale-up to a continuous processing; easy transfer to ceramic industry that commonly applies the spray-drying technology.

The surface potentials of hematite and inert matrix (silica or monoclinic zirconia) have been designed by electroacoustic analysis of their separated slurries. The heterocoagulated mixtures of pigment plus matrix were spray-dried to obtain a new process to get included pigment suitable for ceramic applications.

The colour performances of these included pigments were evaluated by comparison with the matrix/hematite mechanical mixture and the heterocoagulated powder, both dried in a conventional oven. The two-steps process, i.e. heterocoagulation+atomization, is necessary to improve the chemical stability of the included pigment. The hematite colour, in fact, was preserved in both the through-body and low firing glaze applications. In contrast, the mechanical mixture underwent the hematite dissolution in the ceramic media whilst the heterocoagulated powder, though improving the performances of the mechanical mixture, did not reach those of the spray-dried pigments. A calcination at a temperature >900 °C furtherly improves both stability and colour performance of heterocoagulated and spray-dried pigments. The use of silica as inert matrix is not suitable for all ceramic applications: included pigments dissolved in ceramic glazes fired at 1200°C.

The tentative to use ZrO_2 as refractory substitute of SiO_2 indicated that zirconia is not suitable as inert matrix for the inclusion of hematite. In fact, zirconia produces a non-homogeneous coating of hematite. Furthermore, a reaction of ZrO_2 with hematite occurs during ceramic firing, leading to the incorporation of FeO in the baddeleyite crystal lattice, so shifting the colour to gray hues. Nevertheless, further studies regarding alternative inert matrices for higher firing temperatures are in progress.

References

1. Eppler, R.A., Selecting ceramic pigments. *Am. Ceram. Soc. Bull.*, **66**, 1987, 1600-1604.
2. Costa, A.L., Cruciani, G., Dondi, M. & Matteucci, F., New outlooks on ceramic pigments. *Industrial Ceramics*, **23**, 2003, 1-11.
3. Bondioli, F., Manfredini, T. & Pellacani, G.C., Inorganic pigments for ceramic tiles: characteristics and industrial applications. *InterCeram*, **48**, 1999, 414-422
4. Escribano Lòpez, P., Carda Castellò, J.B. & Cordoncillo, C.E., Esmaltes y pigmentos ceràmicos, *Faenza Editrice Iberica*, Castellón, Spain, 2001.
5. Italian Ceramic Society, Colour, pigments and colouring in ceramics, *SALA*, Modena, Italy, 2003.
6. García, A., Llusar, M., Calbo, J., Tena, M.A. & Monrós, G., Low-toxicity red ceramic pigments for porcelainised stoneware from lanthanide–cerianite solid solutions. *Green Chem.*, **3**, 2001, 238-242.
7. Matteucci, F., Cruciani, G., Dondi, M., Baldi, G. & Barzanti, A., Colouring mechanism of red ceramic pigments based on perovskite structure. *Key Eng. Mater.*, **264-268**, 2004, 1549-1552.
8. Lavilla, V.L. & Lopez Rincon, J.M., Study of the mechanism of formation of a zircon-cadmium sulphoselenide pigment. *Br. Ceram. Trans.*, **80**, 1981, 105-108.
9. De Ahna, H.D., Pigments for a new type of ceramic colours, with examples of their applications. *Ceram. Eng. Sci. Proc.*, **1**, 1980, 860-865.
10. Mark, J.E., The sol-gel route to inorganic-organic composites. *Heterogen. Chem. Rev.*, **3**,1996, 307-326.
11. Bondioli, F., Ferrari, A.M., Leonelli, C. & Manfredini, T., Syntheses of Fe_2O_3/silica red inorganic inclusion pigments for ceramic applications. *Mater. Res. Bull.*, **33**, 1998, 723-729.
12. Vicent, J.B., Llusar, M., Badenes, J., Tena, M.A., Vicente, M. & Monrós, G., Occlusion of chromophore oxides by sol-gel methods: application to the synthesis of hematite-silica red pigments. *Bol. Soc. Esp. Ceram. Vidrio*, **39**, 2000, 83-93.
13. Monrós, G., García, A., Sorlí, S., Llusar, M., Calbo, J. & Tena, M.A., Heteromorphic pigment synthesis mechanisms. *Ceram. Acta*, **14** (2), 2002, 12-27.
14. Cava, S., Paskocimas, A., Leite, E.R., Varela, J.A. & Longo, E., Synthesis and encapsulation of cerium-based red pigments. In *Proceedings 7th World Congress on Ceramic Tile Quality - Qualicer*, Castellón, Spain, 2002, Pos. 51-53.
15. Spinelli, A. & Novaes de Oliveira, A.P., Synthesis of a heteromorphic iron oxide red pigment for ceramic application. In *Proceedings 7th World Congress on Ceramic Tile Quality - Qualicer*, Castellón, Spain, 2002, Pos. 245-248.
16. Ricceri, R., Ardizzone, S., Baldi, G. & Matteazzi, P., Ceramic pigments obtained by sol-gel techniques and by mechanochemical insertion of color centers in Al_2O_3 host matrix. *J. Eur. Ceram. Soc.*, **22**, 2002, 629-637.
17. Spinelli, A., Novaes de Oliveira, A.P. & Paskocimas, C.A., Síntese de pigmento cerâmico de óxido de ferro encapsulado em sílica amorfa para aplicações cerâmicas a altas temperaturas (1100-1200 °C). *Cerâmica Industrial*, **8**, 2003, 45-50.
18. Buchner, W., Schliebs, R., Winter, G. & Buchel, K.H., In Industrial inorganic chemistry, *VCH Verlag.*, Weinheim, Germany, 1989, 518-558.
19. Gualtieri, A.F., Natural red pigment for single-fired ceramic glaze. *Am. Ceram. Soc. Bull.*, **81**, 2002, 48-52.
20. Gualtieri, A.F., Different applications of Gres de Thiviers, a red pigment for Traditional ceramics. *Bull. Eur. Ceram. Soc.*, **1**, 2003, 14-18.
21. Albonetti, S., Baldi, G., Bitossi, M., Costa, A.L., Dondi, M., Matteucci, F. & Zama, I., Process for the inclusion of heat-labile ceramic pigments and the inclusion pigments thus obtained. *International Patent WO/2006/100596*, 2006, Colorobbia Italia S.p.A.
22. O'Brien, R.W., Cannon, D.W. & Rowlands, W.N., Electroacoustic determination of particle size and zeta potential. *J. Colloid Interf. Sci.*, **173**, 1995, 406-418.
23. O'Brien, R.W., Electro-acoustic effects in a dilute suspension of spherical particles. *J. Fluid. Mech.*, **190**, 1988, 71-86.
24. O'Brien, R.W., The electroacoustic equations for a colloidal suspension. *J. Fluid. Mech.*, **212**, 1990, 81-93.
25. Larson, A.C. & Von Dreele, R.B., *General Structure Analysis System (GSAS)*. Los Alamos Nat. Lab. Report LAUR, 2000, 86-748.
26. Toby, B.H., EXPGUI, a graphical user interface for GSAS. *J. Appl. Cryst.*, **34**, 2001, 210-213.

27. Gualtieri, A.F., Norby, P., Hanson, J.C. & Hriljac, J., Rietveld refinement using synchrotron X-ray powder diffraction data collected in transmission geometry using an imaging-plate detector: Application to standard m-ZrO_2. *J. Appl. Cryst.*, **29**, 1996, 707-713.
28. Matteucci, F., Lepri Neto, C., Dondi, M., Cruciani, G., Baldi, G. & Boschi, A.O., Colour development of red perovskite pigment $Y(Al,Cr)O_3$ in various ceramic applications. *Adv. Appl. Ceram.*, **105**, 2006, 99-106.
29. Costa, A.L., Bezzi, G., La Torretta, T.M.G. & Verna, S., New process for the preparation of pigment-coated phosphors on the base of electroacoustic characterization. *J. Eur. Ceram. Soc.*, **22**, 2002, 1667-1672.
30. Costa, A.L., Galassi, C. & Greenwood, R., α -Alumina-H_2O interface analysis by electroacoustic measurements. *J. Coll. Interface Sci.*, **212**, 1999, 350-356.
31. Shannon, R.D., Revised effective ionic radii and systematic studies of interatomic distances in halides and chalcogenides. *Acta Crystallogr.*, **A32**, 1976, 751-767.

Table 1
Reagents used in the experiments.

Reagent	Chemical composition	wt. %	Supplier
Hematite	Fe_2O_3	99	Merck, USA
Silica Ludox PX-30 (S.S.A.: 247 m^2/g)	Colloidal SiO_2	30	Grace Davison, USA
Silica Ludox PX-40 (S.S.A.: 165 m^2/g)	Colloidal SiO_2	40	Grace Davison, USA
Silica Ludox PW-50 (S.S.A.: 70 m^2/g)	Colloidal SiO_2	50	Grace Davison, USA
Zirconium hydroxide (S.S.A.: 400 m^2/g)	$Zr(OH)_4$	80-100	Mel, UK
ZrO_2 monoclinic	ZrO_2	99	Mel, UK
Duramax D3021 (additive)	Ammonium polyacrylate	40	Rohm and Haas, USA
Primene JM-T Amine (additive)	Alkyl primary amine	60-100	Rohm and Haas, USA

S.S.A. = specific surface area.

Table 2
Formulation of heterocoagulated suspensions.

Suspension	Total solid content (wt. %)	Inert matrix	Hematite additive	pH
A	30	Ludox PX-30	Primene	3.0
B	30	Ludox PT-40	Primene	3.6
C	30	Ludox PW-50	Primene	3.7
D	40	Ludox PT-40	Primene	4.7
E	30	$Zr(OH)_4$/Primene	Duramax	3.2
F	30	Ludox PX-30	Duramax	3.6

Table 3
Formulation and processing of iron oxide pigments included in silica or zirconia.

Sample	Reagent mixture	Processing
	Silica-coated pigments	
M1	Hematite/amorphous silica powder*	MM
H1	A (Ludox PX-30)	H
S1	A (Ludox PX-30)	H+S
S2	B (Ludox PT-40)	H+S
S3	C (Ludox PW-50)	H+S
S4	D (Solid content 40%)	H+S
C1	A (Ludox PX-30)	H+S+C (950°C)
C2	A (Ludox PX-30)	H+S+C (1100°C)
	Zirconia-coated pigments	
S5	E ($Zr(OH)_4$/Primene)	H+S
M2	Hematite/ZrO_2 (1/25 weight ratio)	MM+C (1300°C)
M3	Hematite/ZrO_2 (1/15 weight ratio)	MM+C (1300°C)

Notes: MM: dry mechanical mixing; H heterocoagulation; S spray-drying; C calcination (maximum firing temperature °C with 200°C/h heating rate and 1 hour of permanence). *Amorphous silica was obtained by drying the Ludox PX-30.

Table 4
Electroacoustic characterization data of the different suspensions.

Sample	Natural pH	Zeta pot. (mV)	Zeta pot. (mV) at pH=3	Zeta pot. (mV) at pH=5	pH_{iep}
Hematite	7.2	+12.8	+36.3	+27.8	9.5
Hematite + Duramax (1.4 wt. %)	7.9	-25.4	-10.0	-20.6	≤ 2
Hematite + Primene (5 wt.%)	9.3	-5.6	+19.4	+15.2	7.7
SiO_2 Ludox PX-30	9.9	-73.3	-10.4	-21.9	≤ 2
SiO_2 Ludox PT-40	8.9	-73.1	+0.4	-14.9	3.3
SiO_2 Ludox PW-50	9.7	-36.8	+0.5	-10.1	4.4
$Zr(OH)_4$	7.3	+7.1	+15.4	+9.9	8.5
$Zr(OH)_4$ + Primene (10 wt.%)	7.8	+14.8	+22.0	+18.8	8.9

Table 5
Rietveld refinements of X-ray diffraction patterns of the zirconia containing samples M2 and M3.

Samples	Goodness of fit R_F^2	Unit-cell volume (Å^3)	Fe occupancy of Zr site (a.p.f.u.)	Isotropic displacement parameters U_{ISO}*100 (Zr,Fe) (Å^2)	Phase composition Fe_2O_3 (% wt.)	Atomic positions x (Zr,Fe)	*y* (Zr,Fe)	*z* (Zr,Fe)
M2	0.02	140.76(5)	0.10(2)	1.1(1)	1.7(2)	.276(1)	.040(1)	.209(1)
M3	0.02	140.88(5)	0.10(2)	1.1(1)	2.5(2)	.275(1)	.040(1)	.209(1)
ZrO_2 [28]	-	140.50(1)	0.00	0.9(1)	0.0	.276(1)	.041(1)	.208(1)

Note: Figures in parentheses are standard deviations on the last decimal figure. R_F^2 is only referred to zirconia reflections.

Figure Captions

Fig. 1. Rietveld refinement plot of the X-ray powder diffraction data of M2 (a) and M3 (b) samples. The continuous line represents the calculated pattern, while cross points show the observed pattern and reflection positions of all the phases are plotted below these patterns. The difference curve between observed and calculated profiles is plotted below.

Fig. 2. Zeta potential vs pH of Ludox sols (A) and of colloidal SiO_2 (●), hematite with Duramax (○) and hematite with Primene (♦) (B).

Fig. 3. Zeta potential of hematite as a function of Duramax added.

Fig. 4. SEM micrographs of hematite pigment included in silica (A) and in zirconia matrices (B).

Fig. 5. Chromatic performances (CIE Lab a*) of SiO_2-containing pigments dispersed in the porcelain stoneware body as a function of firing temperature.

Fig. 6. X-ray powder diffraction patterns of pigments C1 (A) and C2 (B).

Fig. 7 – Effect of SiO_2 surface area on chromatic performances (CIE Lab a*) of pigments dispersed in the porcelain stoneware body as a function of firing temperature. S.S.A(S1) =247m^2/g, S.S.A. (S2)=165 m^2/g , S.S.A.(S3)=70 m^2/g

Fig. 8 – Chromatic performance of pigments applied into the glassy coating F: CIE a* vs. L* (A) and a* vs. b* (B).

Fig. 9 – Chromatic performance of pigments applied into the ceramic glaze G: CIE a* vs. L* (A) and a* vs. b* (B).

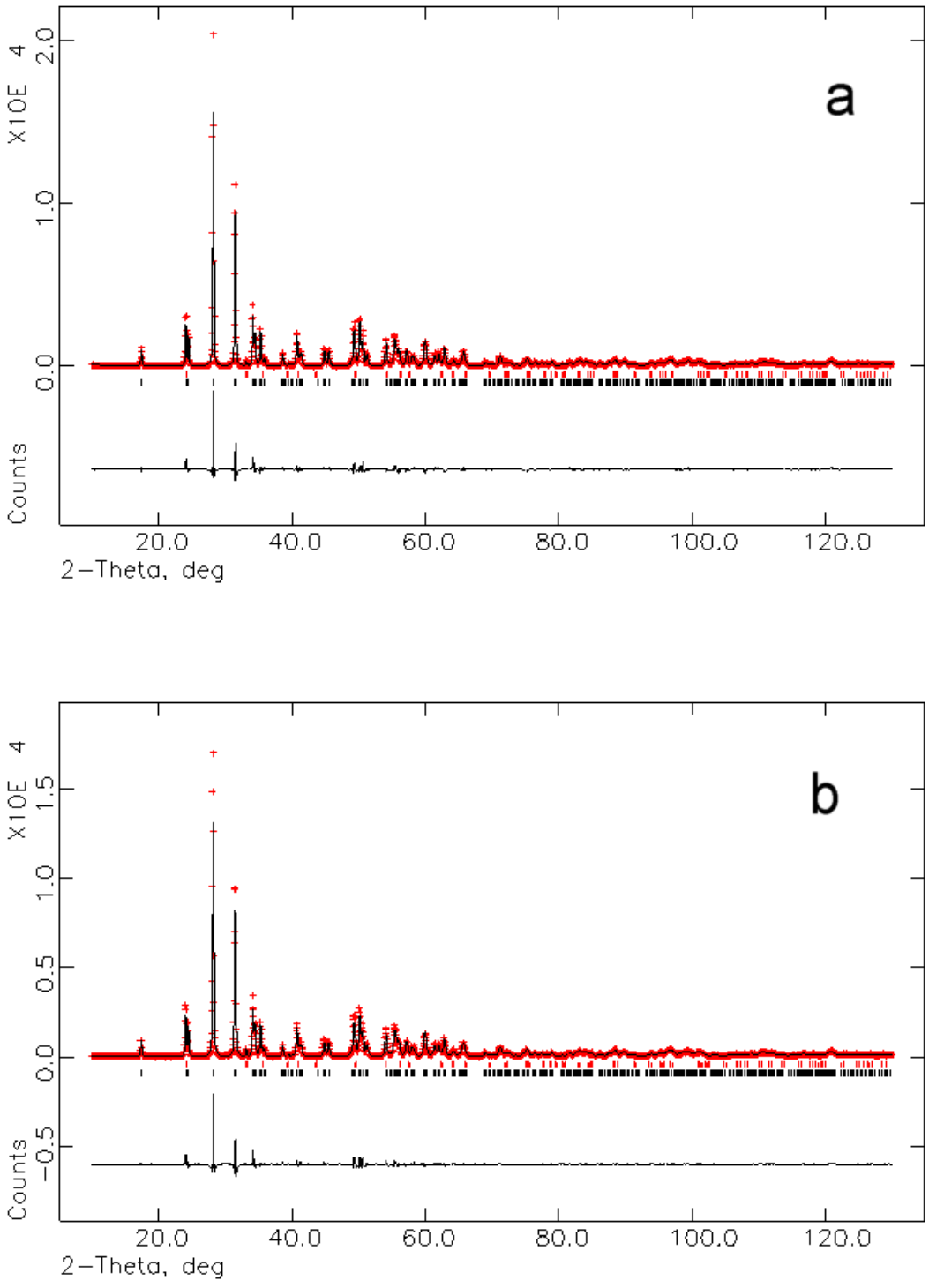

Fig. 1. Rietveld refinement plot of the X-ray powder diffraction data of M2 (a) and M3 (b) samples. The continuous line represents the calculated pattern, while cross points show the observed pattern and reflection positions of all the phases are plotted below these patterns. The difference curve between observed and calculated profiles is plotted below.

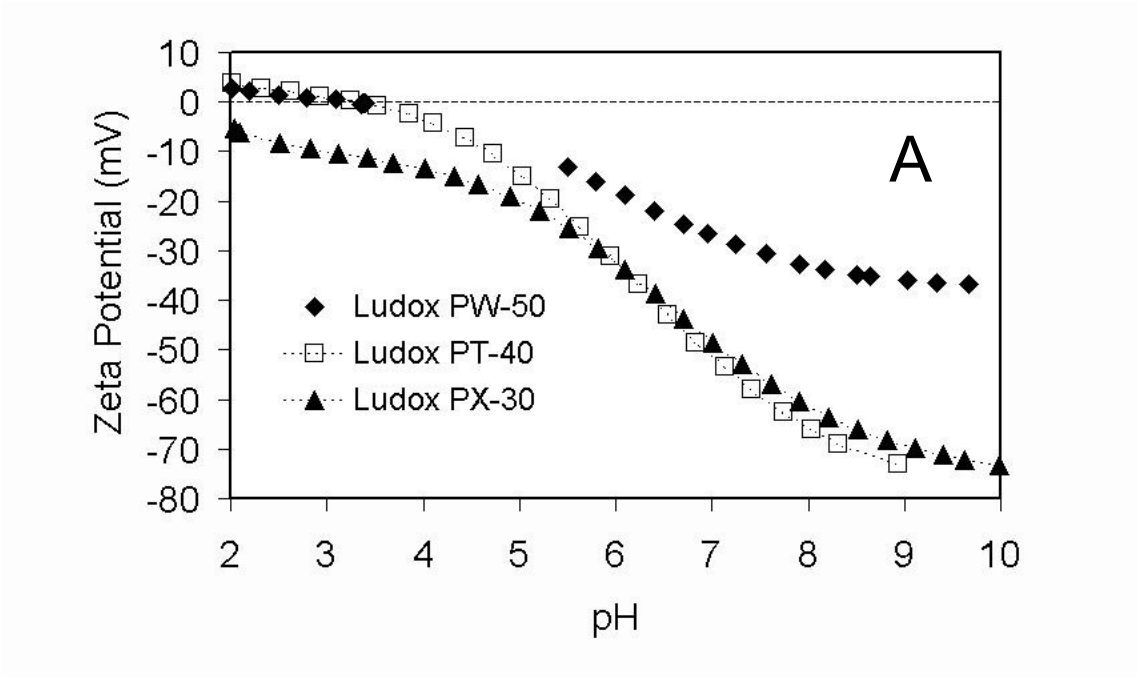

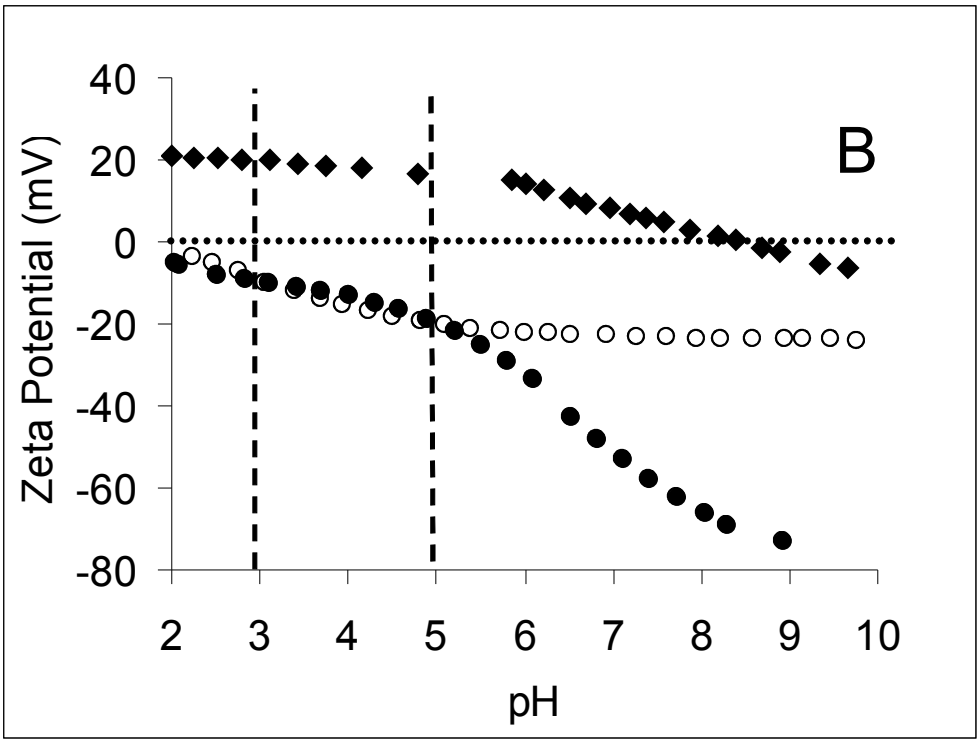

Fig. 2. Zeta potential vs pH of Ludox sols (A) and of colloidal SiO_2 (●), hematite with Duramax (○) and hematite with Primene (♦) (B).

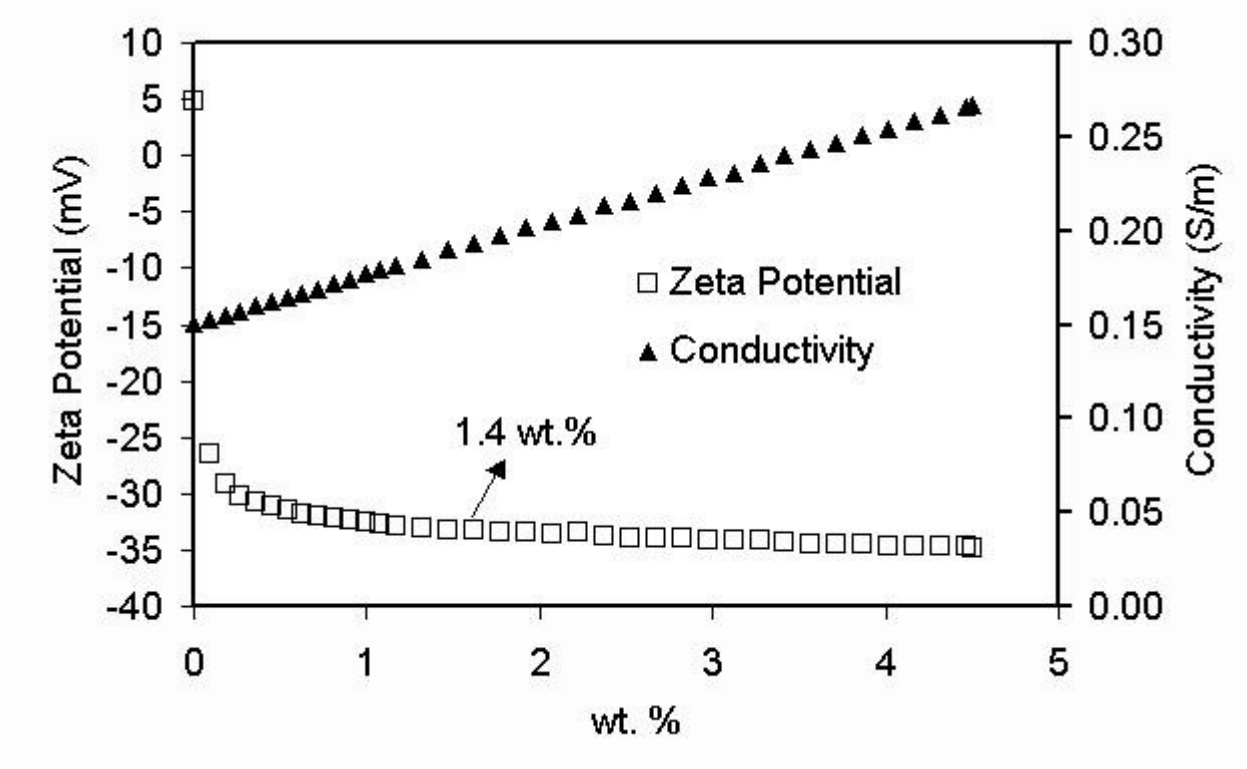

Fig. 3. Zeta potential of hematite as a function of Duramax added.

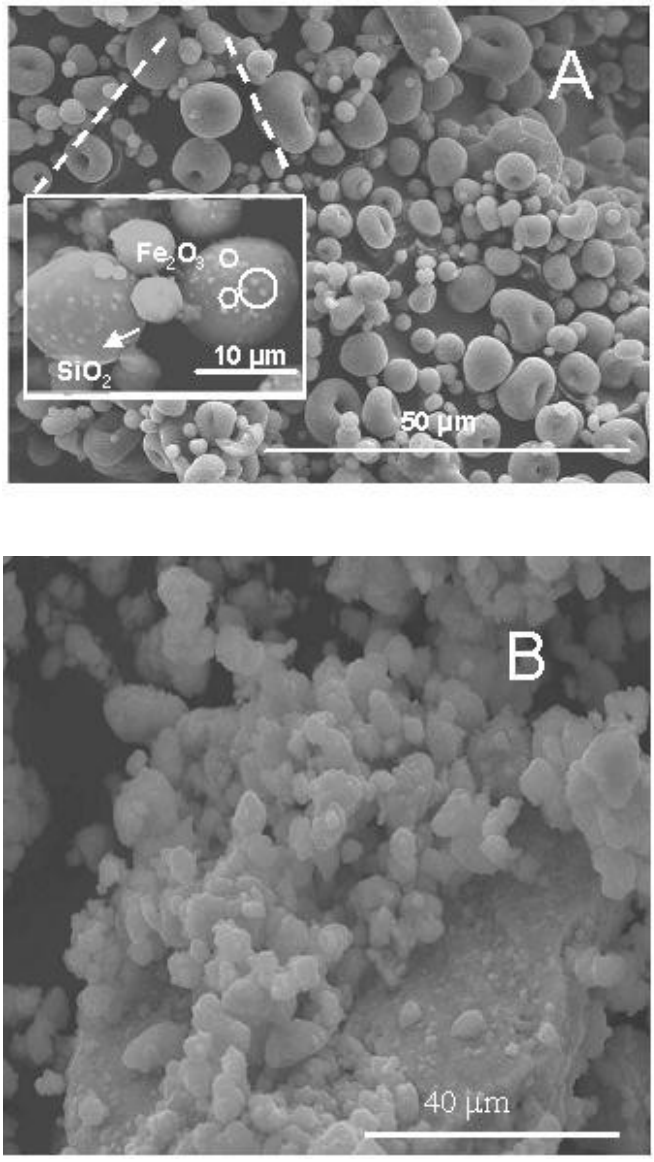

Fig. 4. SEM micrographs of hematite pigment included in silica (A) and in zirconia matrices (B).

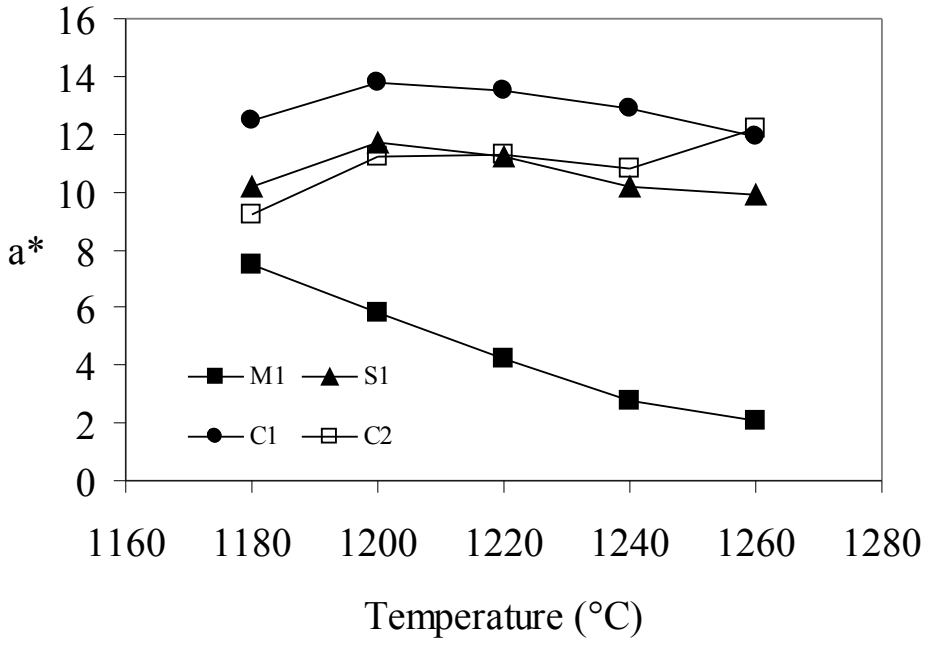

Fig. 5. Chromatic performances (CIE Lab a*) of SiO_2-containing pigments dispersed in the porcelain stoneware body as a function of firing temperature.

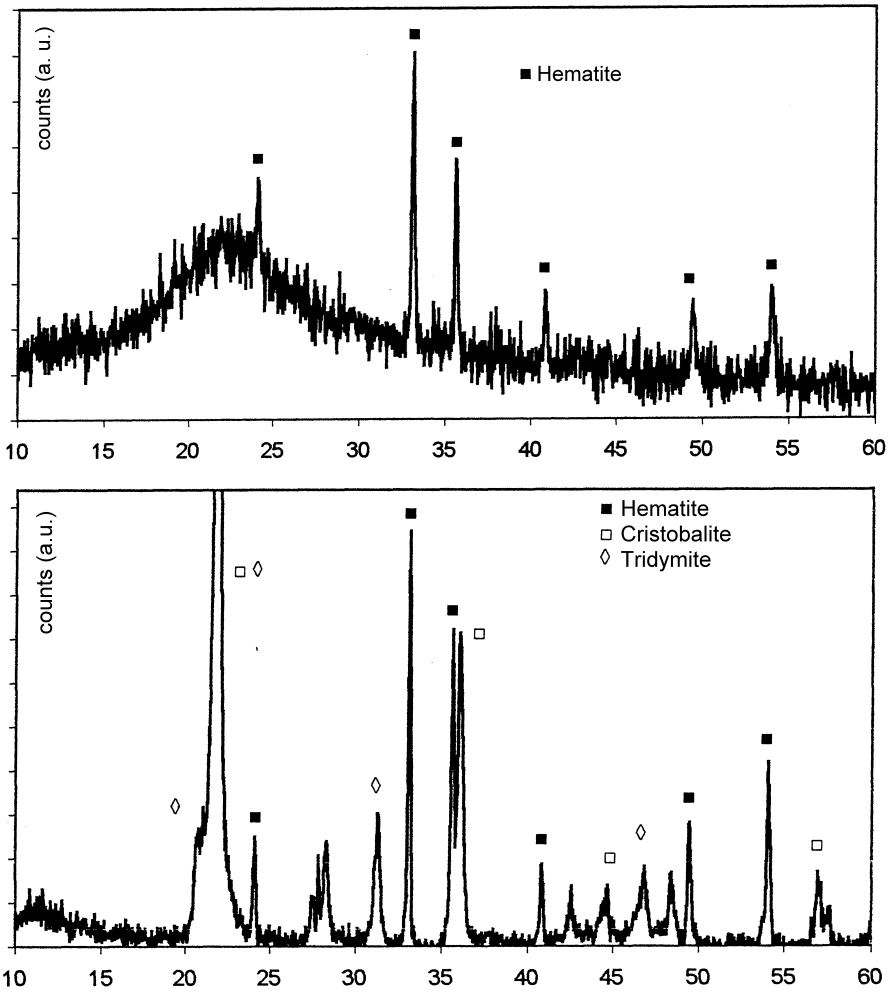

Fig. 6. X-ray powder diffraction patterns of pigments C1 (A) and C2 (B).

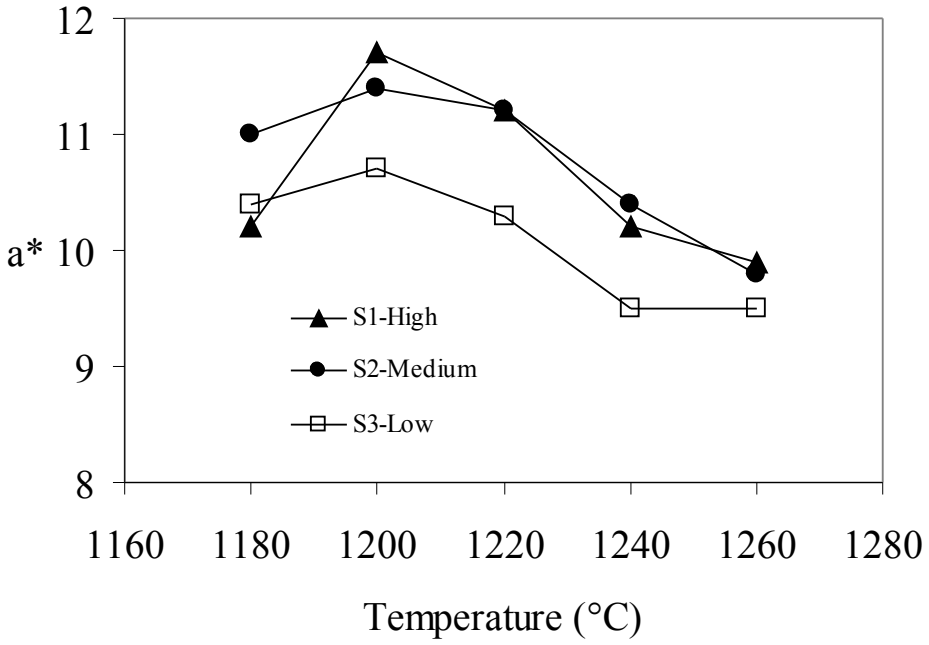

Fig. 7 – Effect of SiO_2 surface area on chromatic performances (CIE Lab a*) of pigments dispersed in the porcelain stoneware body as a function of firing temperature. S.S.A(S1) =247m^2/g, S.S.A. (S2)=165 m^2/g , S.S.A.(S3)=70 m^2/g

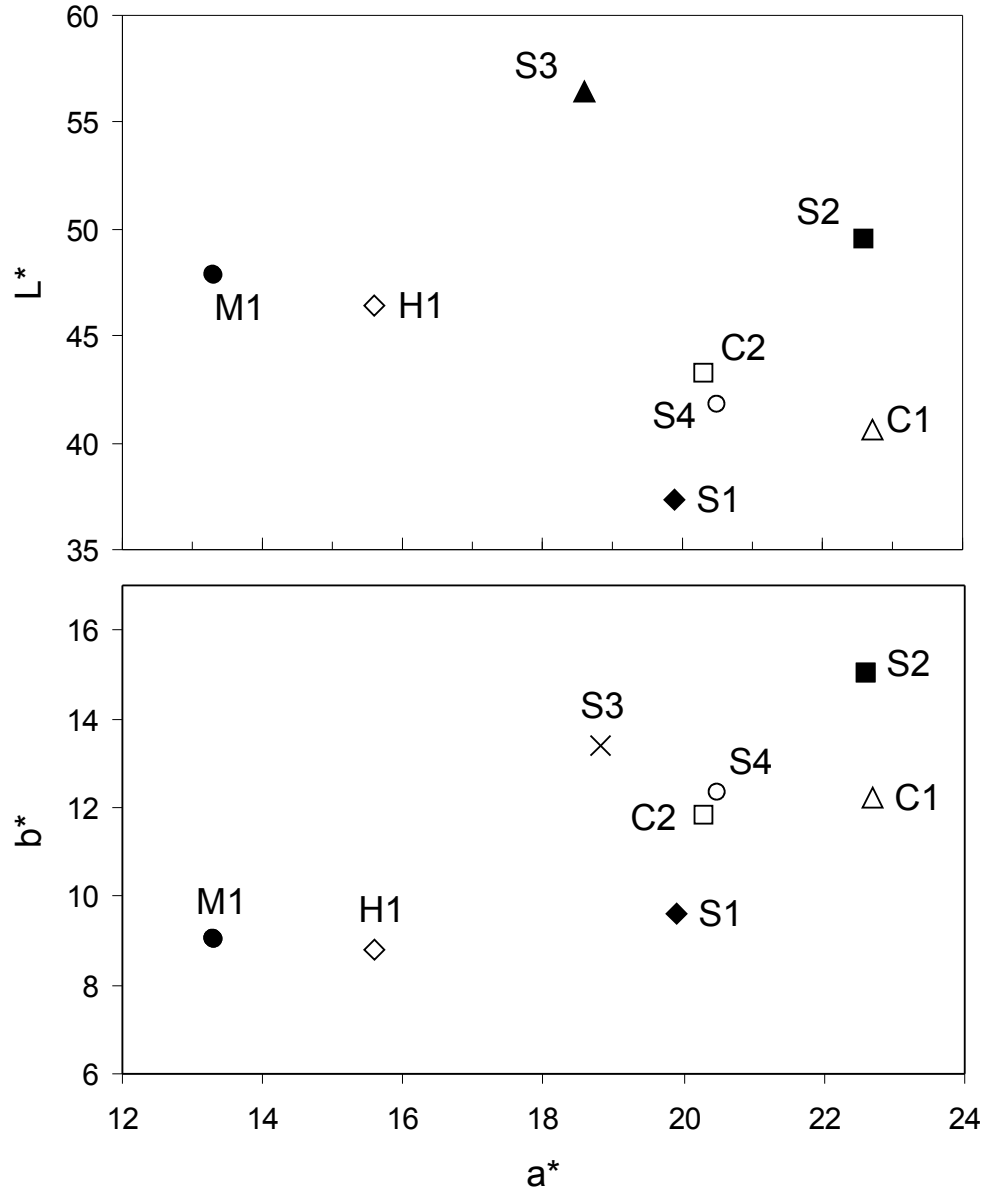

Fig. 8 – Chromatic performance of pigments applied into the glassy coating F: CIE a* vs. L* (A) and a* vs. b* (B).

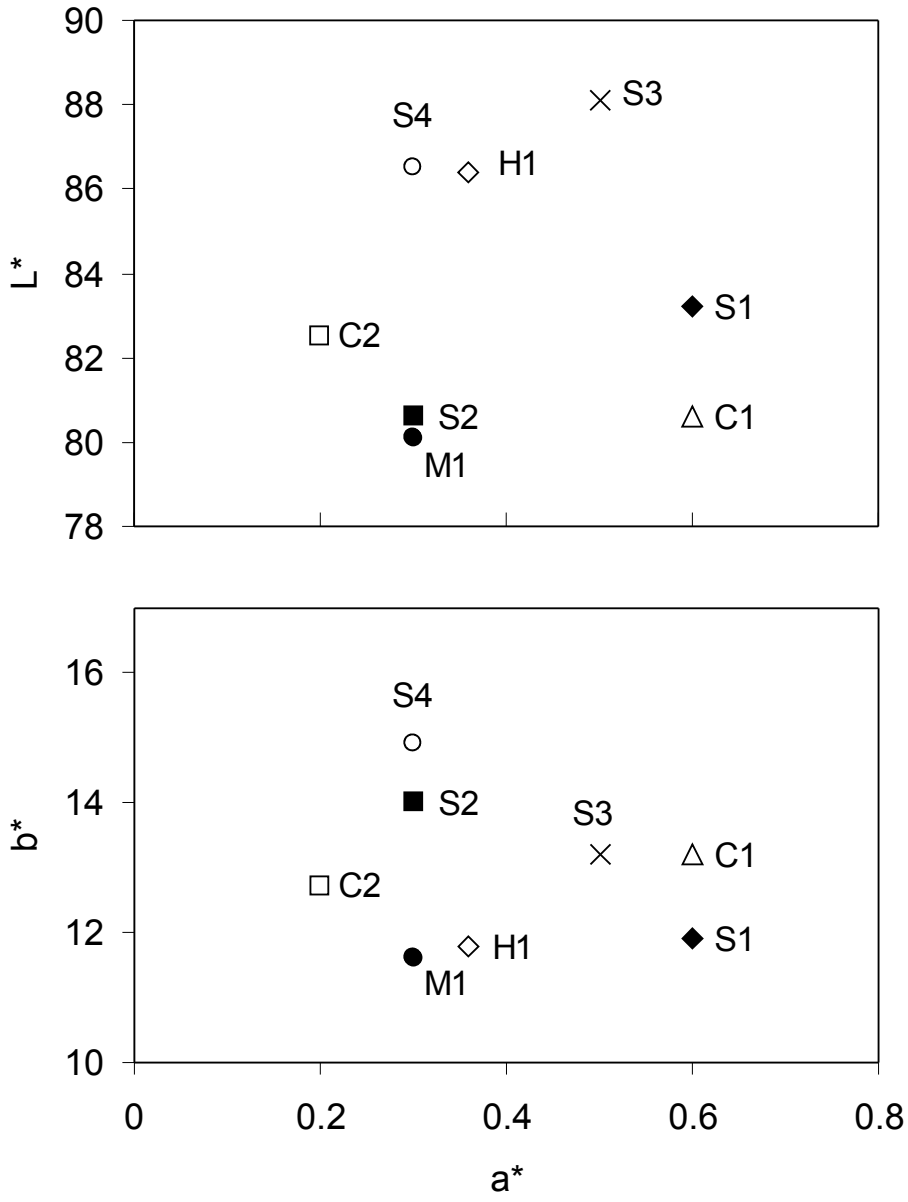

Fig. 9 – Chromatic performance of pigments applied into the ceramic glaze G: CIE a* vs. L* (A) and a* vs. b* (B).